A COMPUTER CODES PACKAGE FOR ELECTRON TRANSPORT MONTE CARLO SIMULATION

LUCREȚIU M. POPESCU

Environmental Radioactivity Laboratory, Institute for Environmental Research and Engineering, Spl. Independenței 294, 77703 Bucharest, Romania

Received September 3, 1998

A computer codes package was developed for solving various electron transport problems by Monte Carlo simulation. It is based on condensed history Monte Carlo algorithm. In order to get reliable results over wide ranges of electron energies and target atomic numbers, specific techniques of electron transport were implemented such as: Molière multiscatter angular distributions, Blunck-Leisegang multiscatter energy distribution, sampling of electron-electron and bremsstrahlung individual interactions. Path-length and lateral displacement corrections algorithms and a module for computing collision, radiative and total restricted stopping powers and ranges of electrons are also included. Comparisons of simulation results with experimental measurements are finally presented.

1. INTRODUCTION

The simplest approach of application of the Monte Carlo method to radiation transport problems is the analogue simulation in which random trajectories of the particles with the medium are generated according to the probability distributions governing each individual interaction. This analogue method to be desirable for computer simulation is required to have few interactions per particle history, that is the case for photons or neutrons, but not for electrons. Due to the enormous number of collisions (long range Coulomb interactions) encountered by electrons, analogue simulation of electron transport is possible only in a few exceptional cases. Therefore most electron transport algorithms use condensed-history techniques in which the electron is traced in a series of steps, and multiple scattering theories are used to group individual scattering events which occur during each step. This makes electron transport more complex, first form the point of view of underlying physics of the simulations, and second from the point of view of the complexity of the algorithm and computational aspects.

A Monte Carlo simulation code has four major components: (1) the cross-section data for all processes being considered in the simulation, (2) the algorithms used for the particle transport, (3) the methods used to specify the geometry of the problem and to determine quantities of interest, and (4) the analysis of the infor-

mation obtained during the simulation. While the last two components have an important contribution to the complexity of computer code and running time, only the first two are relevant from the point of view of the underlying physics of the simulation, therefore we intend to describe hereby only these aspects.

2. THE ALGORITHM

According to the classification operated by Berger [1] condensed history Monte Carlo schemes can be divided into two broad categories, called class I and class II. These are classified according to how they treat individual events that lead to major changes of the particle properties. In class I models, the energy losses and angular deflections associated with all individual interactions are grouped together and the changes in energy and direction of the primary electron

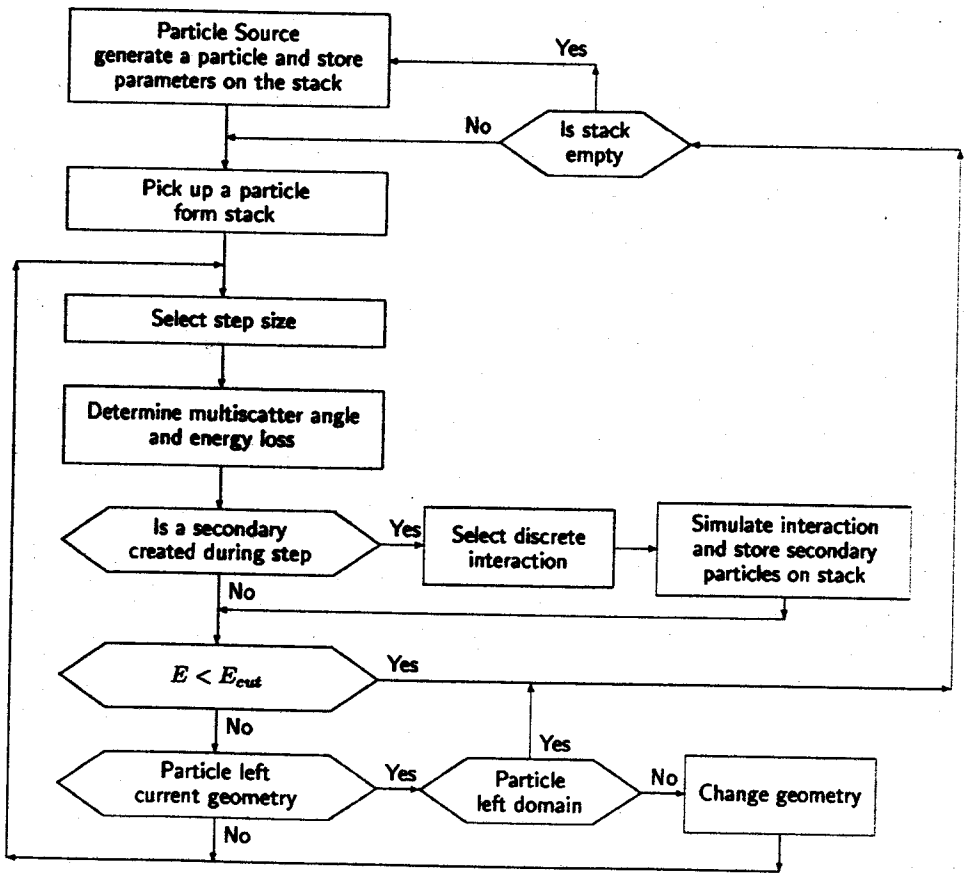

Fig. 1. – Flow chart of class I condensed history Monte Carlo particle transport algorithm.

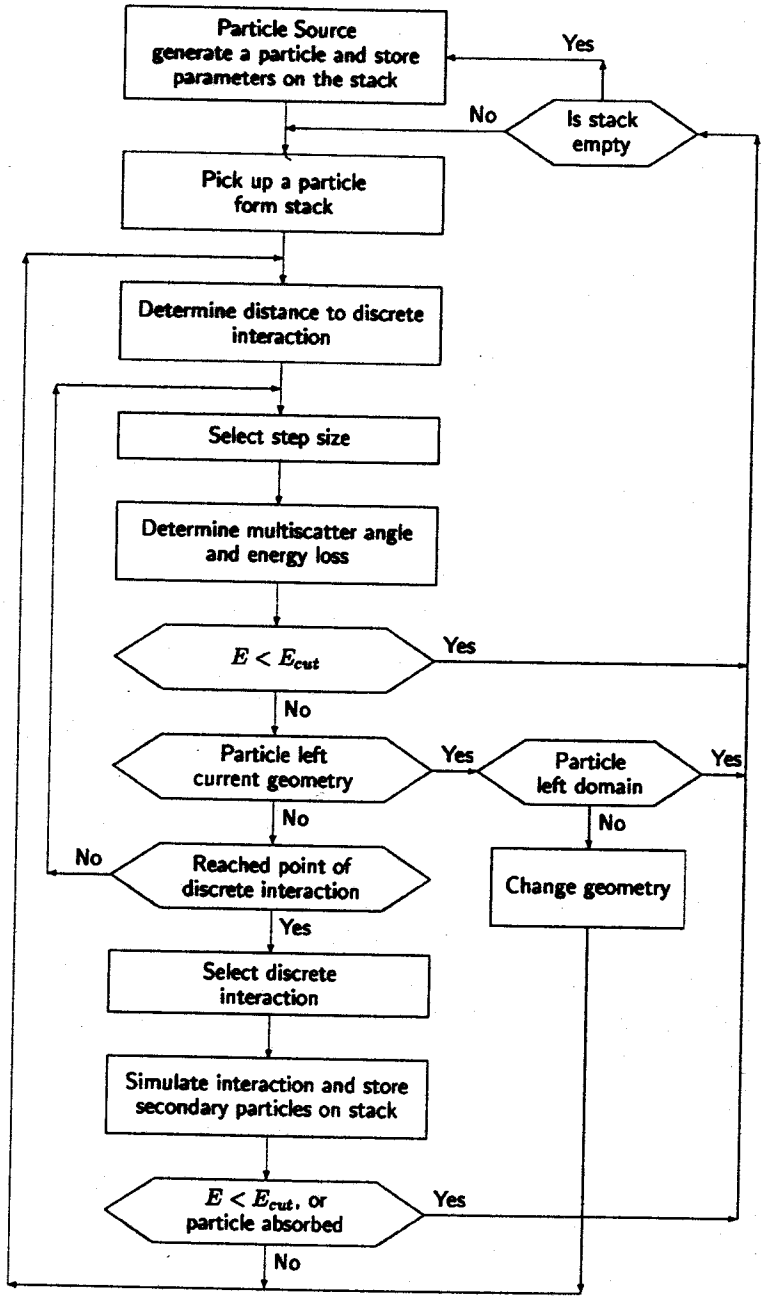

Fig. 2. – Flow chart of class II condensed history Monte Carlo particle transport algorithm.

are not correlated with the creation of individual secondary particles. In class II models the collisions in which the particle loses a large fraction of its energy,

above certain energy thresholds, are simulated as individual interactions and only the remaining interactions are treated in a continuous manner.

In this computer code package routines which allow the construction of condensed history schemes of both classes were implemented. The algorithm corresponding to the class I condensed history model is outlined in Fig. 1 while an algorithm specific to the condensed history schemes of class II is presented in Fig. 2.

2.1. PRODUCTION OF KNOCK-ON ELECTRONS

The discrete events considered are production of knock-on electrons and creation of bremsstrahlung photons. The production of knock-on electrons is simulated using the Møller differential cross section of electron-electron interaction.

$$\frac{d\Sigma_{Møller}(T_0)}{dT} = \frac{2\pi n r_0^2 m_0 c^2}{\beta^2 T_0}\left[C_1 + \frac{1}{\varepsilon}\left(\frac{1}{\varepsilon} - C_2\right) + \frac{1}{\varepsilon'}\left(\frac{1}{\varepsilon'} - C_2\right)\right], \tag{1}$$

where: T_0 is the initial electron kinetic energy; T is the final electron kinetic energy; T' is the kinetic energy taken by the secondary electron; $\varepsilon = T/T_0$, $\varepsilon' = T'/T_0$; and $C_1 = [(\gamma-1)/\gamma]^2$, $C_2 = (2\gamma-1)/\gamma^2$. β, γ are usual relativistic factors of incident electron; n is electron density; r_0 is the classic electron radius, and m_0c^2 is the electron rest energy.

The minimum kinetic energy of the secondary electron is denoted by T_E, because of the identity of final electrons, by convention we call secondary electron that which has the final energy in the interval $(T_E, T_0/2)$ and the scattered electron is that with energy in the interval $(T/2, T_0 - T_E)$. Due to introduction of the cut off energy T_E, the energy threshold for discrete Møller scattering is $2T_E$.

The angular deflections of scattered and secondary electrons are obtained from momentum conservation laws of two body interactions.

2.2. PRODUCTION OF BREMSSTRAHLUNG

For the simulation of bremsstrahlung interaction, the formula proposed by Al-Beteri and Raeside [2] and their efficient algorithm for random sampling of individual radiative interactions were used. This formula was obtained by adding corrections to Bethe-Heitler integral cross section formula through a fit to experimental bremsstrahlung cross section data, and predictions of it exhibit better agreement with experimental values than other existing bremsstrahlung cross section over wide ranges of electron energies (1 MeV $\leq T \leq$ 250 MeV) and target atomic numbers ($4 \leq Z \leq 82$).

$$\frac{d\sigma}{d\varepsilon} = 4\alpha r_0^2 Z(Z+\delta)\frac{1}{\varepsilon}\left[1+(1-\varepsilon)^2-\frac{2}{3}(1-\varepsilon)\right]\times \left[\Phi(\xi, Z)+F_1(\beta, Z)+F_2(\beta_0, Z)-\frac{1}{3}\ln Z\right], \quad (2)$$

where: E_0 is total energy of incident electron; k is the energy of bremsstrahlung photon; $E = E_0 - k$ is total of electron after interaction; $\varepsilon = k/E_0$, $\gamma_0 = E_0/m_0c^2$, $\gamma = E/m_0c^2$, $\beta_0^2 = 1-1/\gamma_0^2$, $\beta^2 = 1-1/\gamma^2$ are usual relativistic factors; $\delta = 0.75$ is a correction term introduced to include bremsstrahlung emission in the field of atomic electrons; and α is the fine structure constant ($\approx 1/137$). The corrections functions are:

$$\Phi(\xi, Z) = 4.6\left(1+1/Z^2\right)-(1/\beta_0)\ln(\xi+\beta_0-0.3),$$
$$F_1(\beta, Z) = \alpha Z(1-\beta^5),$$
$$F_2(\beta_0, Z) = 0.5\left(\alpha Z/\gamma_0\beta_0\right)^2;$$

where $\xi = \dfrac{100m_0c^2Z}{E_0}\dfrac{\varepsilon}{1-\varepsilon}$ is the screening parameter.

After interaction the direction of electron remains unchanged.

From the above formula, relations for computing the bremsstrahlung restricted stopping power and restricted cross-section, required in the preparation part of the simulation algorithm, were analytically derived [3].

2.3. CONTINUOUS ENERGY LOSS

The energy loss in the continuous energy loss approximation is computed using adequate stopping power formulas (average energy loss per track length). For a particular kind of interaction the stopping power is obtained solving the integral

$$-\frac{dE}{dx} = \int_0^{W_{max}} \frac{d\Sigma}{dW}\,dW, \quad (3)$$

where W_{max} is the maximum energy loss considered. In class I models W_{max} is equal to the maximum energy allowed by physical laws, while in class II models it is set to lower values, to exclude the interaction with large energy losses from the group of continuous slowing down interaction, since these events are treated separately.

The total stopping power is composed from collisional stopping power, which includes excitation and ionization processes, and bremsstrahlung stopping power.

$$\left(\frac{dE}{dx}\right)_{total} = \left(\frac{dE}{dx}\right)_{coll} + \left(\frac{dE}{dx}\right)_{brem}.$$

The collisional stopping power used is that proposed initially by Bethe with corrections added by Bloch and Sternheimer. According to Seltzer and Berger [4] for restricted collisional stopping power we have the relation

$$\left(-\frac{dE}{dx}\right)_{coll} = \frac{2\pi n r_0^2 m_0 c^2}{\beta^2}\left[\ln\frac{2(\tau+2)}{(I/m_0c^2)^2} + f^-(\tau,\Delta) - \delta\right] \tag{4}$$

with:

$$f^-(\tau,\Delta) = -1-\beta^2 + \ln[(\tau-\Delta)\Delta] + \tau/(\tau-\Delta) + \left[\frac{\Delta^2}{2} + (2\tau+1)\ln\left(1-\frac{\Delta}{\tau}\right)\right]\frac{1}{\gamma^2}, \tag{5}$$

where: $\gamma = E_0/m_0c^2$, $\tau = \gamma - 1$, $T'_E = T_E/m_0c^2$, $T'_{\max}$ is maximum energy to be transferred, $\tau/2$ for electrons, $\Delta = \min(T'_E, T'_{\max})$ is maximum energy transferred, δ is density effect correction which is introduced using the Sternheimer approach [5].

Bremsstrahlung restricted stopping power formula was determined from the integral (3) with Al-Beteri and Raeside cross section (2) [3].

During the simulation process it is necessary to determine the average distance traversed by electron when it loses a given energy, or having a distance to be traversed to determine the average energy loss. This is done by solving the integral for the electron range,

$$R(T) = \int_0^T \frac{1}{\left(-\frac{dE}{dx}\right)(T')}\,dT'. \tag{6}$$

The above equation is solved numerically for an energy grid and after that the range for an arbitrary energy is determined by linear interpolation.

The average distance ΔR traversed by an electron with initial kinetic energy T_0 which loses the energy ΔT is given by:

$$\Delta R = R(T_0) - R(T_0 - \Delta T). \tag{7}$$

As $R(T)$ is a monotonic increasing function it can be inverted. The inverse function $T(R)$ represents the energy which must have the electrons to travel the average distance R until they are stopped. The average energy loss when the distance ΔR is passed is given by:

$$\Delta T = T_0 - T(R_0 - \Delta R), \tag{8}$$

where $R_0 = R(T_0)$.

In condensed history class II models, another required quantity, computed in the preparation part of the simulation, is:

$$Q(T) = \int_{T_{min}}^{T} \Sigma(T') \left(-\frac{dE}{dx} \right)^{-1} dT', \tag{9}$$

where $\Sigma(T)$ is the total macroscopic cross section of the discrete events considered. It can be interpreted as the number of discrete interactions per track length, and it is used to determine the distance to the next discrete interaction given by the random sampling relation [1]:

$$\Delta Q = -\ln \varsigma, \tag{10}$$

where ΔQ is the variation of $Q(T)$ until the next point of discrete interaction is reached, and ς is a random number uniformly distributed in the interval (0, 1).

$Q(T)$ is computed numerically using the same energy grid as in the case of $R(T)$. Subsequently are also obtained by interpolation between grid points the relationships $Q(R)$ and $R(Q)$. Together with equations (7) and (8) the distance to the next discrete interaction point is given by

$$\Delta R = R(Q_0) - R(Q_0 - \Delta Q), \tag{11}$$

where $Q_0 = Q(T_0)$ and $R(Q_0) = R(T_0)$.

2.4. ENERGY LOSS FLUCTUATIONS

For constructing a class I condensed history algorithm an option is to introduce energy loss fluctuations after traversing an energy step. Blunck and Leisegang [6] refined the formula obtained by Landau [7] proposing the following relationship for the energy loss ΔT of electrons with initial kinetic energy T_0 traversing a slab of thickness x, losing the average energy $\overline{\Delta T}$:

$$f_{BL}(\Delta T) = \sum_{i=1}^{4} \frac{c_i \gamma_i}{\sqrt{b^2 + \gamma_i^2}} \exp\left[-\frac{(\lambda - \lambda_i)^2}{b^2 + \gamma_i^2} \right] \frac{d\lambda}{d(\Delta T)}, \tag{12}$$

where:

$$\lambda = \frac{\Delta T - \overline{\Delta T}}{ay} + \ln\left(\frac{T_0}{ay} \right) - 1.116;$$

$y = x\rho$ – mass thickness of the slab (g/cm^2);

$$a = 0.154 \frac{Z}{A} \frac{1}{\beta^2};$$

$$b = \sqrt{q\overline{\Delta T}} \cdot \frac{Z^{\frac{2}{3}}}{ay}$$

$q \approx 20\,\text{eV}$ – arbitrary energy which affects mainly the tail ends of the distribution,

$c_i, \lambda_i, \gamma_i, i = \overline{1,4}$ – constants tabulated in table 1.

Table 1

Values of constants used in Blunck-Leisegang distribution function taken from [17].

	$i=1$	$i=2$	$i=3$	$i=4$
c_i	0.174	0.058	0.019	0.007
λ_i	0.00	3.00	6.50	11.00
γ_i	1.80	2.00	3.00	5.00

Blunck-Leisegang distribution is valid for $\overline{\Delta T} \ll T_0$. Generally it is a good agreement with experimental measurements, but for low energies large discrepancies are observed [8], in addition the results are significantly sensitive to steps sizes chosen.

For class II condensed history models some fluctuations of energy loss are already introduced since they treat distinctly the interaction which leads to large energy losses. But for studies of electrons traversing thin slabs, the energy spectrum obtained is dependent on energy thresholds chosen for discrete interactions. To avoid this it is necessary to introduce a restricted energy loss distribution formula, in which only the interactions below these thresholds are included. An option is the use of a gaussian distribution [9]

$$f(T_0, \Delta T, x) = \frac{1}{\sqrt{2\pi\rho^2 x}} e^{\frac{(\Delta T - \overline{\Delta T})}{2\rho^2 x}}, \tag{13}$$

where

$$\rho^2 = \int_0^{W_{max}} W^2 \frac{d\Sigma(W)}{dW} dW. \tag{14}$$

In our calculations we evaluated ρ^2 using the Møller electron-electron cross section formula (1), with $W_{max} = T_E$.

2.5. DETERMINATION OF MULTIPLE-SCATTER ANGLE

The electron multiple-scattering on atomic nuclei is treated using the Molière [10, 11] theory with corrections of Bethe [12]. This theory given the

angular distributions as the series

$$f(\theta)\theta\,d\theta = \vartheta\,d\vartheta\left[f^{(0)}(\vartheta)+\frac{1}{B}f^{(1)}(\vartheta)+\frac{1}{B^2}f^{(2)}(\vartheta)+\ldots\right] \tag{15}$$

$$f^{(n)}(\vartheta)=\frac{1}{n!}\int_0^\infty J_0(\eta\vartheta)e^{-\frac{\eta^2}{4}}\left(\frac{\eta^2}{4}\ln\frac{\eta^2}{4}\right)^n \eta\cdot d\eta\,,$$

where

$$\vartheta=\frac{\theta}{\chi_c\sqrt{B}}, \tag{17}$$

is the reduced angle, J_0 is the zero-order Bessel function and B and χ_c are defined by the equations:

$$B-\ln B=\ln\Omega_0, \tag{18}$$

$$\chi_c=\chi_{cc}\frac{\sqrt{s}}{\beta^2 E}, \tag{19}$$

where b_c and χ_{cc} are constants which depend only on the medium in which the transport takes place. Ω_0 can be interpreted as the number of atomic collisions that contribute to the scattering and is related to the step length by the equation

$$\Omega_0=\frac{b_c s}{\beta^2}, \tag{20}$$

For elements:

$$b_c=6702.33\frac{\rho Z^{\frac{1}{3}}(Z+\xi)}{A}\cdot\frac{1}{1+0.000178\cdot Z^2}\,[\mathrm{cm}^{-1}], \tag{21}$$

$$\chi_{cc}=0.39612\sqrt{\frac{\rho Z(Z+\xi)}{A}}\,[\mathrm{MeV}\cdot\mathrm{cm}^{-1/2}], \tag{22}$$

where ρ is the density in g/cm^3, s is the step length in cm, Z is the atomic number of the element, and A is the atomic mass in atomic mass units. E is the electron total energy in MeV, and ξ is a correction term introduced to take into account the inelastic scatterings with atomic electrons and usually taken equal to unity; an additional correction to χ_{cc} is given by Fano [13].

In eq. (16) for $n = 0$ we have a gaussian curve:

$$f^{(0)}(\vartheta)=2e^{-\vartheta^2}, \tag{23}$$

but for $n \geq 1$ Molière functions must be computed using numerical methods. Terms until of order two proved to be sufficiently accurate. In the sampling algorithm used by us, Molière functions were taken from [14].

Molière considered his theory valid for $\Omega_0 > 20$. Originally derived as a small-angle theory, Molière multiple-scattering theory has been modified by Bethe to predict accurately large-angle scattering by multiplying the right side of eq. (15) with a correction term $\sqrt{\theta/\sin\theta}$. The minimum step size $s_{\min}$ required to ensure sufficient number of scatterings is given by:

$$s_{\min} = \frac{\Omega_0 \beta^2}{b_c} \text{ [cm]}, \tag{24}$$

with $\Omega_0 = 20$, while the maximum step size derived by Bethe is

$$s_{\max} = \frac{E^2\beta^4}{\chi_{cc}\ln(b_c E^2\beta^2/\chi_{cc})} \text{ [cm]}. \tag{25}$$

The polar multiple-scatter angles is taken randomly in the interval $[0, 2\pi]$.

2.6. ELECTRON SPATIAL DISPLACEMENT AFTER MULTIPLE SCATTERINGS

Let us consider an electron with initial coordinate $\vec{r}_0$ and momentum versor $\vec{u}_0$. The simplest way to determine the new position ($\vec{r}$) is to assume that the electron trajectory is a straight line

$$\vec{r} = \vec{r}_0 + s \cdot \vec{u}_0. \tag{26}$$

In reality the trajectory has a disordered form and the final position is expected to be correlated with the final deflection angles (θ, φ). In the particle coordinate system let us denote with $(\Delta x, \Delta y, \Delta z)$ the spatial displacement of electron after traversing the step. Berger [1] has proposed for the longitudinal displacement the simple formula

$$\Delta z = \frac{s}{2}(1 + \cos\theta). \tag{27}$$

The lateral displacement can be evaluated in the small angle approximation using gaussian distributions [9]:

$$\begin{aligned} \Delta x &= \frac{s}{2}\left(\sin\theta\cos\varphi + g_x\sqrt{\frac{1-\langle\cos\theta\rangle}{3}}\right), \\ \Delta y &= \frac{s}{2}\left(\sin\theta\sin\varphi + g_y\sqrt{\frac{1-\langle\cos\theta\rangle}{3}}\right), \end{aligned} \tag{28}$$

where g_x and g_y are standard normal random variables and $\langle\cos\theta\rangle$ is the average

of deflection angle cosine. The resultant lateral displacement $\Delta r_\perp = \sqrt{\Delta x^2 + \Delta y^2}$, has the average:

$$\overline{\Delta r_\perp} = \frac{s}{2}\sin\theta . \tag{29}$$

When Δx and Δy are sampled using the formula (28) the values for which $\Delta x^2 + \Delta y^2 + \Delta z^2 > s^2$ obviously must be rejected, but this is found to be most unlikely. It should be mentioned that the introduction of lateral displacements leads to an ambiguity in the determination of the exit point when the electron left the geometry; therefore near boundaries a special treatment with smaller steps sizes must be used.

3. COMPARISON WITH EXPERIMENTAL BENCHMARKS

Electron transport Monte Carlo codes are very complex and use a large amount of cross section data. Simulation results are also influenced by different parameters, dependent on particles energies and materials, introduced in construction of algorithms to control the simulation of electrons histories. Therefore it is essential to evaluate Monte Carlo codes by comparing calculated data with high-quality experimental data in order to eliminate coding errors, to help refine algorithms, and, most important, to estimate systematic uncertainties associated with approximations in the codes.

For meaningful comparisons between calculations it is preferable to have high-quality data in very simple configurations. Unfortunately, it is often very difficult to find experimental data which are of sufficiently high quality, or have a simple enough configuration. Another complicating factor is that certain experimentally measured quantities are poor indicators of the overall accuracy of all components of a calculation: *i.e.* good agreement with experiment for some calculated quality does not verify the accuracy of the entire calculation.

Table 2

Summary of electron transmission and angular distribution simulations.

Material	Incident energy [MeV]	Thickness		Transmision Coefficient	
		[g/cm²]	fraction of range	Measured	Monte Carlo
Aluminum	1	0.10	0.2	0.98	0.94
	2.5	0.31	0.2	0.90, 0.97[a]	0.98
Gold	1	0.15	0.2	0.43	0.43
	2.5	0.37	0.2	0.48	0.50

[a] Transmission factor measured by Miller [18].

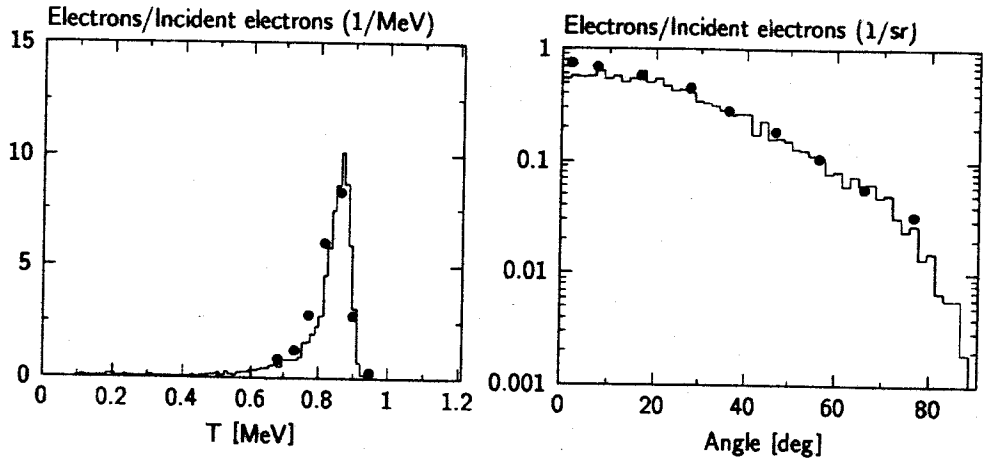

Fig. 3. – Transmitted electrons energy and angular distribution for 1 MeV incident electrons perpendicular on 0.10 g/cm^2 of aluminum.

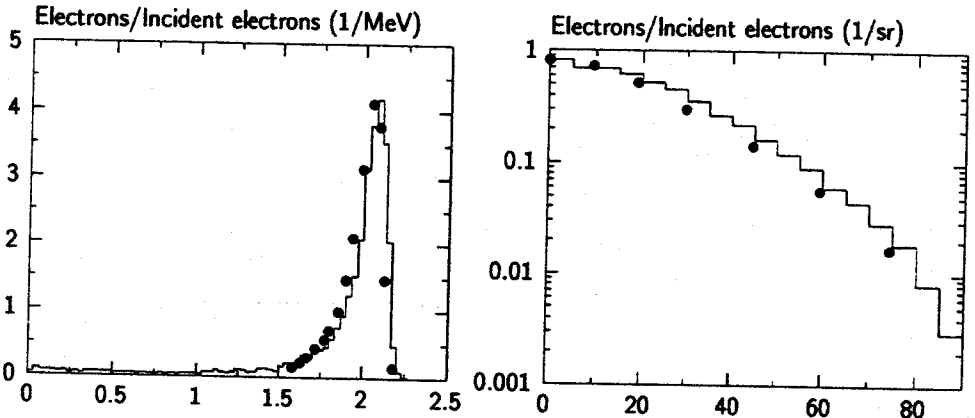

Fig. 4. – Transmitted electrons energy and angular distributions for 2.5 MeV incident electrons perpendicular on 3.61 g/cm^2 of aluminum.

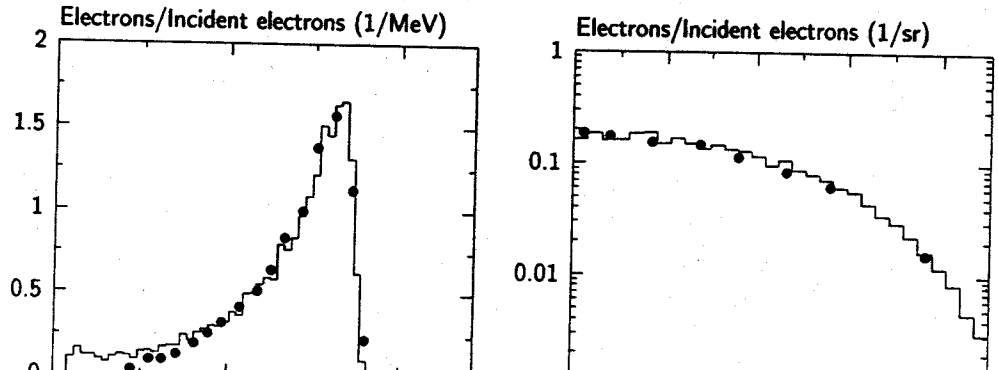

Fig. 5. – Transmitted electrons energy and angular distributions for 1 MeV incident electrons perpendicular on 0.15 g/cm^2 of gold.

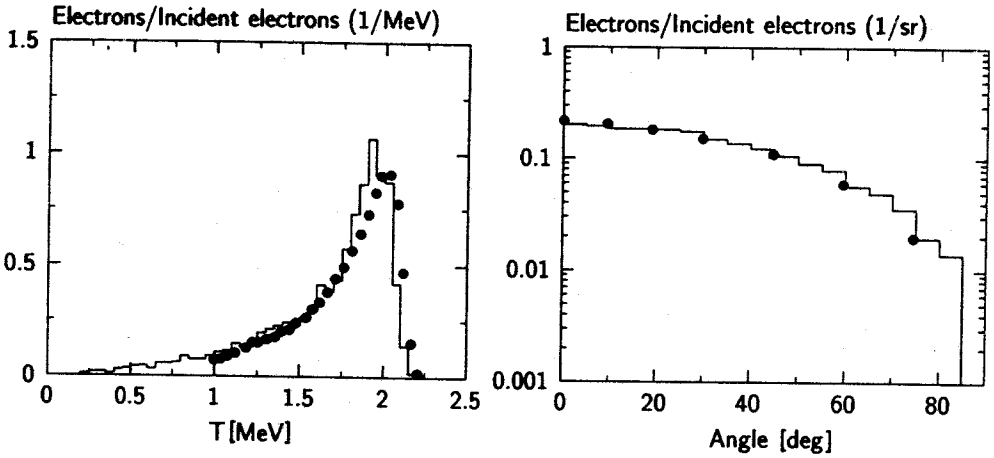

Fig. 6. – Transmitted electrons energy and angular distributions for 2.5 MeV incident electrons perpendicular on 0.37 g/cm^2 of gold.

For a first series of comparisons were used measurements of Rester and Derrickson [15] of electron transmission energy spectra and angular distributions in aluminum and gold at bombarding energies of 1.0 and 2.5 MeV. The simulation carried out are summarized in table 2. Comparison of calculated data with experimental measurements are presented in Fig. 3, 4, 5 and 6.

One of the most frequently utilization of Monte Carlo calculations are done for dose calculations, therefore another series of test simulations was done for comparisons with depth-dose distributions. Such comparisons are presented in Fig. 7, 8 and 9 where the measurements are taken from [16].

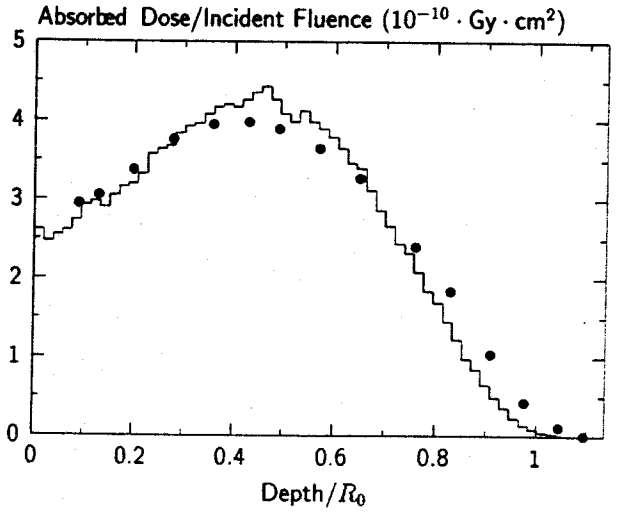

Fig. 7. – Depth-dose curve for 1 MeV electrons incident normally on a thick target of beryllium. The bullets represent experimental data of [19] taken from [16]. The depth scale is given relative to electrons CSDA-range at incident energy.

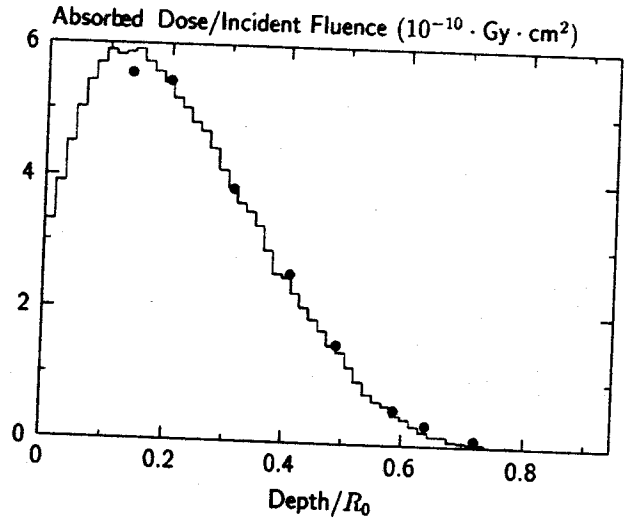

Fig. 8. – Same as in Fig. 7 but for 1 MeV electrons incident normally on a thick target of copper.

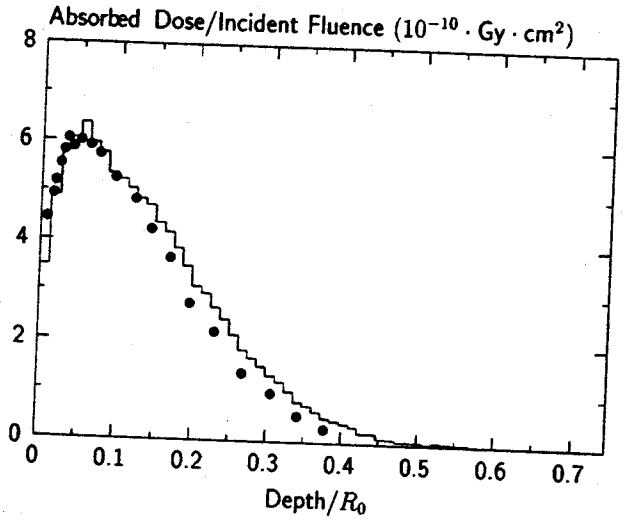

Fig. 9. – Same as in Fig. 7 but for 1 MeV electrons incident normally on a thick target of uranium.

In all above cases were performed a large enough number of electron histories simulation in order to decrease the statistical uncertainties to the level of measurements uncertainties.

4. CONCLUSION

A computer codes package for electron transport Monte Carlo simulation was developed. Routines which implement specific electron transport simulation techniques are included in order to facilitate construction of both class I and II

condensed history on schemes. Comparisons of simulation against simple configurations experimental benchmarks reveal a good agreement.

Acknowledgements. The author expresses his thanks to Prof. Octavian Sima, from Physics Department of Bucharest University and to Prof. Mircea Oncescu from Institute of Atomic Physics, for their support, and suggestions in revising the manuscript.

REFERENCES

1. M. J. Berger, *in Methods in Computational Physics* (Adler, B., Fernbach, S., Rotenberg, M., editors) volume 1, Academic Press, New York 1963 135–215.
2. A. A. Al-Beteri, D. E. Raeside, *Nucl. Inst. Meth. Phys. Res.*, **B44**, 149 (1989).
3. L. M. Popescu, *Romanian Journal of Physics*, **41** (7–8) (1996) 527–535.
4. M. J. Berger, S. M. Seltzer Report NBSIR 82-2550, U. S. Departament of Comerce, National Bureau of Standards, Washington, SUA, 1982.
5. R. M. Sternheimer, *Phys. Rev.*, **103**, 511 (1956).
6. O. Blunck, S. Leisegang, *Z. Phys.*, **128**, 500 (1950).
7. L. D. Landau, *Journal of Physics of USSR*, **8**, 257 (1944).
8. C. T. Ballinger, D. E. Cullen, S. T. Perkins, J. A. Rathkopf, W. R. Martin, S. J. Wilderman, *Nucl. Inst. Meth. Phys. Res.*, **B72**, 19–27 (1992).
9. B. Rossi, K. Greisen, *Rev. Mod. Phys.*, **13**, (1941) 240–309.
10. G. Z. Molière, *Z. Naturforsch*, **2a**, 133 (1947).
11. G. Z. Molière, *Z. Naturforsch*, **3a**, 78 (1948).
12. H. A. Bethe, *Phys. Rev.*, **89** (6), 1256 (1953).
13. U. Fano, *Phys. Rev.*, **93**, 117 (1954).
14. O. Sima, Personal comunication, (1993).
15. D. H. Rester, J. H. Derrickson *Journal of Applied Physics*, **42**(2) (1971) 714–721.
16. D. W. O. Rogers, A. F. Bielajew, *in The Dosimetry of Ionizing Radiation* (K. R. Kase, B. E. Bjärngard, F. H. Attix, editors) volume III, Academic Press, 1990 chapter 3, 427–539.
17. O. Sima, *Simularea Monte Carlo a transportului radiațiilor*, Editura All, București, (1994).
18. E. Miller Technical Report TN D 5724, NASA, 1970 citation in [15].
19. G. J. Lockwood, G. J. Ruggles, L. E. Miller, J. A. Halbleib, Technical Report 79-0414, Sandia National Laboratories, Albuquerque, New Mexico, USA, 1980.